



**Simulated coordinated impacts of the NAO and El Niño on
aerosol concentrations over eastern China**

Juan Feng¹, Jianping Li^{1,2}, Hong Liao³, and Jianlei Zhu⁴

1. *College of Global Change and Earth System Science, Beijing Normal University, Beijing,*

China

2. *Laboratory for Regional Oceanography and Numerical Modeling, Qingdao National*

Laboratory for Marine Science and Technology, Qingdao, China

3. *School of Environmental Science and Engineering, Nanjing University of Information Science*

& Technology, Nanjing, China

4. *China-ASEAN Environmental Cooperation Center, Beijing, China*

Corresponding author:

Dr. Juan Feng

College of Global Change and Earth System Science (GCESS),

Beijing Normal University, Beijing 100875, China

Tel: 86-10-58802762

Email: fengjuan@bnu.edu.cn



Abstract

The high aerosol concentrations (AC) over eastern China have attracted attention from both science and society. Based on the simulations of a chemical transport model using a fixed emissions level, the possible role of the previous autumn North Atlantic Oscillation (NAO) combined with the simultaneous El Niño-South Oscillation (ENSO) on the boreal winter AC over eastern China is investigated. We find that the NAO only manifests its negative impacts on the AC during its negative phase over central China, and a significant positive influence on the distribution of AC is observed over south China only during the warm events of ENSO. The impact of the previous NAO on the AC occurs via an anomalous sea surface temperature tripole pattern by which a teleconnection wave train is induced that results in anomalous convergence over central China. In contrast, the occurrence of ENSO events may induce an anomalous shift in the western Pacific subtropical high and result in anomalous southwesterlies over south China. The anomalous circulations associated with a negative NAO and El Niño are not favorable for the transport of AC and correspond to worsening air conditions. The results highlight that the combined effects of tropical and extratropical systems play considerable role in affecting the boreal winter AC over eastern China.



41 **1. Introduction**

42 Atmospheric particles (i.e., aerosols) are the key pollutants that exhibit an
43 important adverse impact on human health, environmental pollution, global climate
44 change, and atmospheric visibility (IPCC, 2013). Aerosol particles may alter the
45 precipitation rates and optical properties of clouds (Hansen et al., 1997), impacting the
46 radiation balance of the entire Earth-atmosphere system via absorbing and scattering
47 solar radiation (Jiang et al., 2017; Yue and Unger, 2017). A better understanding of
48 aerosol variations is therefore important and useful for scientific and social endeavors.

49 The meteorology parameters, i.e., atmospheric temperature (Aw and Kleeman,
50 2003; Liao et al., 2015), boundary layer (Kleeman, 2008; Yang et al., 2016), wind (Zhu
51 et al., 2012; Yang et al., 2014, 2017), and humidity (Ding and Liu, 2014), show a non-
52 negligible impact on the regional aerosol concentrations (AC) via affecting the
53 deposition and transportation processes. Moreover, the intraseasonal and interannual
54 variations in climatic phenomena could affect both the spatial and temporal
55 accumulation and distribution of AC due to the associated variations in the circulation
56 and rainfall anomalies. For example, the monsoon onset could affect the seasonal
57 variations in regional AC (Tan et al., 1998; Chen and Yang, 2008). The interannual
58 variation of AC over East Asia is connected with the interannual variation of East Asian
59 winter monsoon (Jeong and Park, 2016; Lou et al., 2016, 2018; Mao et al., 2017) and
60 summer monsoon (EASM; Zhang et al., 2010; Zhu et al., 2012). The seasonal evolution
61 of the El Niño-South Oscillation (ENSO) impacts the seasonal variations of AC over
62 northern and southern China (Liu et al., 2013; Feng et al., 2016a). The AC variation in



63 the US is influenced by the Pacific Decadal Oscillation (Singh and Palazoglu, 2012).
64 These findings suggest that the role of climate systems in impacting the regional air
65 quality cannot be ignored.

66 The North Atlantic Oscillation (NAO), reflecting large scale fluctuations in
67 pressure between the subpolar low and subtropical high, is one of the most determinant
68 and influential climate variability modes in the extratropical Atlantic Ocean, (e.g.,
69 Hurrell, 1995; Gong et al., 2001; Visbeck et al., 2001). A negative (positive) polarity of
70 the NAO is reflected by positive (negative) pressure anomalies over the high latitudes
71 of the North Atlantic and negative (positive) pressure anomalies over the central North
72 Atlantic. Both the positive and negative phases of NAO are accompanied with large
73 scale modulations in the location and intensity of the North Atlantic jet stream and
74 storm track (Gong et al., 2001; Li and Wang, 2003). The surface layer wind would vary
75 associated with changes in the jet stream because of the NAO's quasi-barotropic
76 characteristic, resulting in varied Ekman heat transport and basin-wide variations in the
77 underlying sea surface temperatures (SST; Marshall et al., 2001; Wu et al., 2009).

78 The NAO massively impacts the temperature and precipitation patterns over the
79 US and central Europe, i.e., a wet and warm winter in Europe, and mild and wet winter
80 conditions would be expected accompanied with a positive NAO phase. Moreover, the
81 NAO exhibits significant cross-seasonal impacts on the East Asian climate. For
82 example, it is reported that variation in boreal spring NAO influenced the subsequent
83 intensity of the EASM from 1979-2006 (Wu et al., 2009). The linkage between the
84 EASM and NAO has been further explored by Zuo et al. (2013) but on the interdecadal



85 scale, and it is suggested that the preceding spring NAO dominated the relationship of
86 the NAO-EASM more than the simultaneous summer NAO, similar result is seen in
87 Zheng et al. (2016). Xu et al. (2013) presented that the previous boreal summer NAO
88 significantly influenced the following September rainfall over central China. These
89 studies highlight the important role of the NAO signal on the climate in East Asia,
90 especially the cross-seasonal impacts, which are beneficial for seasonal forecasting.

91 In addition to the influence of the extratropics, the impact originating from the
92 tropics is another important driver of the climate anomalies in China. As the most
93 dominant interannual variability of the tropical air-sea coupled system, the El Niño-
94 Southern Oscillation (ENSO) exhibits profound influences on the weather and climate
95 around the world (e.g., Ropelewski and Halpert, 1987; Harrison and Larkin, 1998). The
96 occurrence of ENSO phenomenon displays significant effects in impacting the global
97 and regional oceanic and atmospheric anomalous patterns (e.g., Rasmusson and
98 Carpenter, 1982; Trenberth, 1997). The seasonal climate variation in China is closely
99 linked with the evolution of ENSO events. For example, increased rainfall is expected
100 to be found over the Huai-he and Yangtze River valley, whereas less rainfall is seen
101 over northern and southern China during the decaying summer of an El Niño event
102 (Zhang et al., 1996, 1999). During the developing autumn of an El Niño event,
103 enhanced rainfall would be expected over southern China due to the associated
104 anomalous shift in the western Pacific subtropical high (WPSH). However, without
105 significant influence during the developing summer (Feng et al., 2016b).



106 As shown above, both the NAO and ENSO significantly impact the climate over
107 China. China now suffering from relatively high aerosol loading, and this is commonly
108 ascribed to the increased emissions connected with the speedy economic growth.
109 However, as discussed above that the role of meteorological conditions in affecting the
110 AC cannot be ignored. Accordingly, it is of interest to explore the possible impacts of
111 the NAO and ENSO on the distributions of AC over China. The possible impacts of the
112 NAO on the aerosol has been discussed by Moulin et al. (1997) and Jerez et al. (2013);
113 however, they concentrated on its influences on the North Atlantic Ocean and Europe,
114 respectively. Feng et al. (2016a) indicated the potential effects of El Niño on the AC
115 over China, but with a focus on the seasonal evolution. Therefore, does the NAO exhibit
116 significant impacts on the AC, and how the combination of the NAO and ENSO affect
117 the distribution of AC over China, as both of them show important modulation of the
118 climate over China.

119 The above discussions provide the main motivation of the present work. The
120 conditions in boreal winter are discussed in the present work, as this time is
121 corresponding to the heat supply season and the AC over China peak during this season.
122 The coordinated role of the previous autumn (September to November, SON) NAO and
123 the simultaneous ENSO is compared to that of the NAO alone, and also as well as the
124 involved physical mechanisms. The rest of this paper is arranged as follows. Model,
125 datasets, and methodology employed are presented in Section 2. The possible impacts
126 of the NAO and ENSO on the AC are explored in Section 3. Section 4 discusses the
127 involved physical mechanism. Section 5 provides the discussion and conclusions.



128 **2. Datasets, simulations, and methodology**

129 **2.1 Datasets**

130 The input background meteorological variables of the GEOS-Chem model show
131 high degree of uniformity with the current widely used reanalyses (e.g., Zhu et al., 2012;
132 Yang et al., 2014). Here, the SLP in the National Centers for Environmental
133 Prediction/National Center for Atmospheric Research (NCEP/NCAR) reanalysis
134 (Kalnay et al., 1996) with a 2.5° latitude \times 2.5° longitude resolution, and the UK
135 Meteorological Office Hadley Centre's sea ice and SST datasets (HadISST; Rayner et
136 al., 2003) with a 1° latitude \times 1° longitude resolution are used to verify the reliability
137 of the Goddard Earth Observing System, Version 4 (GEOS-4).

138 **2.2 GEOS-Chem simulations**

139 The influences of the NAO on the simulated AC over China are examined using a
140 three-dimensional tropospheric chemistry model, i.e., GEOS-Chem (version 8.02.01;
141 Bey et al., 2001). The model is driven by assimilated meteorological fields from the
142 GEOS-4 of the NASA Global Modeling and Assimilation Office, with a 2° latitude \times
143 2.5° longitude resolution, and 30 hybrid vertical levels. This model contains a detailed
144 coupled treatment of tropospheric ozone-NO_x-hydrocarbon chemistry, as well as
145 aerosols and their precursors, containing nitrate, black carbon, sulfate, sea salt,
146 ammonium, mineral dust, dust aerosols, and organic carbon (Bey et al., 2001; Liao et
147 al., 2007). The aerosol dry and wet depositions follow Wesely (1989) and Liu et al.



(2001), with details in Wang et al. (1998). According to Liao et al. (2007), the AC were defined as PM_{2.5} as follows,

$$[PM_{2.5}] = 1.37 \times [SO_4^{2-}] + 1.29 \times [NO_3^-] + [POA] + [BC] + [SOA] \quad (1)$$

SO_4^{2-} , NO_3^- , POA, BC, and SOA are the aerosols particles of sulfate, nitrate, primary organic aerosol, black carbon, and second organic aerosol, respectively. The sea salt aerosols and mineral dust are not considered for that measurements indicate that they are not the major aerosol species in the eastern China during winter (Xuan et al., 2000; Duan et al., 2006).

The anthropogenic emissions in the GEOS-Chem and experiment design are similar to Zhu et al. (2012), in which the biomass burning emissions and anthropogenic emissions are fixed at year 2005 level in the simulation. That is the observed variations in the distributions of AC as seen below was due to the variations in meteorological conditions associated with climate events. Due to the longevity of the GEOS-4 datasets, the period 1986-2006 is focused on. GEOS-Chem is a well-recognized atmospheric chemistry model and is widely utilized due to its capability to well characterize the seasonal, interannual, and decadal variations of pollutant aerosols in the East Asia and beyond (e.g., Zhu et al., 2012; Yang et al., 2014, 2016). The well performance and wide application of GEOS-Chem provide confidence for employing the model to investigate the coordinated impacts of NAO and El Niño on the AC over eastern China.

2.3 NAO index and Niño3 index



168 The NAO index (NAOI) is employed to quantify the variations in the NAO phase
 169 (Hurrell et al., 1995; Gong and Wang, 2001). The definition of the NAOI follows Li and
 170 Wang (2003) and is calculated as the zonal mean SLP difference between 35°N (i.e.,
 171 refers to the mid-latitude center) and 65°N (i.e., refers to the high latitude center) from
 172 80°W to 30°E over the North Atlantic by

$$173 \quad \text{NAOI} = \hat{P}_{35^{\circ}\text{N}} - \hat{P}_{65^{\circ}\text{N}} \quad (2)$$

174 where P is the monthly mean SLP averaged from 80°W to 30°E, \hat{P} is the normalized
 175 value of P , and the subscripts indicate latitudes. For a given month m in year n , the
 176 normalization \hat{P} is defined as follows

$$177 \quad \hat{P}_{n,m} = \frac{P'_{n,m}}{S_P} \quad (3)$$

178 where $P'_{n,m}$ is the monthly pressure anomaly of $P_{n,m}$, departure from period 1986-
 179 2006, and S_P is the total standard deviation of the monthly anomaly $P'_{n,m}$,

$$180 \quad S_P = \sqrt{\frac{1}{12 \times 21} \sum_{i=1986}^{2006} \sum_{j=1}^{12} P_{j,i}'^2} \quad (4)$$

181 The monthly NAOI is calculated based on the monthly mean SLP from both the
 182 NCEP/NCAR and GEOS-4 assimilated meteorological dataset for 1986-2006. The
 183 boreal autumn NAOI is defined as the average of the monthly NAOI during September,
 184 October, and November (Fig. 1). The series of NAOI show strong interannual variations,
 185 and the two series based on GEOS-4 and NCEP/NCAR are closely correlated with each
 186 other with a significant coefficient of 0.98, implying the GEOS-4 dataset could capture
 187 the variation in the NAO.



188 El Niño events were defined as standardized 3-month running mean Niño3 index
189 (areal mean SST averaged over 150°-90°W, 5°N-5°S) above 0.5°C and persisting for at
190 least 6 months. The skin temperature (i.e., SST over ocean and surface air temperature
191 on land) was employed to obtain the Niño3 index for that SST is not available in the
192 GEOS-4 meteorological dataset. The boreal winter Niño3 index is calculated as the
193 average of the monthly Niño3 during December, January, and February, i.e., winter
194 1997 is for the December 1997 and January and February 1998. The boreal winter
195 Niño3 indices based on the GEOS-4 and HadISST are significantly correlated with each
196 other, (Fig. 1), with a coefficient of 0.99. The high correlations among the indices
197 further indicate the reliability of the model data.

198 **3. Influences of the NAO and El Niño on the AC over China**

199 **3.1 Climatological Characteristics of the AC**

200 The spatial distribution of the standard deviation of boreal winter AC is shown in
201 Fig. 2. Eastern China (105°E eastward, 35°N southward) shows high loading of
202 aerosols in both the column and surface layer concentrations (figure not shown). Further,
203 the variance of winter AC over eastern China is most pronounced compared to other
204 regions during this season (Fig. 2a, b). As an evident monsoonal region, eastern Asia is
205 influenced by winter monsoon, i.e., a strong Aleutian low is seen in the north Pacific,
206 and the Asian continent is controlled by the Siberian high during boreal winter. The
207 strong pressure gradient between the Siberian high and Aleutian low results in strong
208 northwesterlies prevailing over eastern China (Fig. 2c).



209 **3.2 Relationships between the AC & NAO and El Niño**

210 The spatial distribution between the surface AC and previous autumn NAOI and
211 simultaneous winter Niño3 index are presented in Fig. 3. Positive correlations are seen
212 over south China (30°N south) in the correlations with the Niño3 index, indicating that
213 a warm ENSO event would associate with high AC over south China. In contrast,
214 negative correlations over south and central China are observed in the correlations with
215 autumn NAO, implying a positive NAO phase is linked with less AC over these regions,
216 thus favoring better air conditions. The analysis suggests that the ENSO and NAO show
217 opposite effects on AC over south China, i.e., the NAO displays a negative impact and
218 the ENSO displays a positive impact. However, the relationship between the autumn
219 NAOI and winter Niño3 index is insignificant with a correlation of -0.08 during period
220 1986-2006.

221 The above relationships are further examined in their positive and negative phases,
222 as strong asymmetry was reported in the climatic impacts of the NAO (Xu et al., 2013;
223 Zhang et al., 2015) and ENSO (Cai and Cowan, 2009; Karior et al., 2013; Feng et al.,
224 2016b). The asymmetric influences of the NAO and ENSO on AC are obvious in the
225 spatial distributions of the linear correlation coefficients (Fig. 4). During the El Niño
226 events, south China is impacted by significant positive correlations, in contrast, a non-
227 significant correlation is observed over this region during the La Niña events. This point
228 implies the significant relationships between the ENSO and AC over south China are
229 mainly connected with warm events, i.e., El Niño. The negative correlations between
230 the NAO and AC mainly occurred in the negative phase of the NAO, and the significant



231 correlations are mainly located in central China (lie from 28°N to 40°N). Thus, the
232 ENSO affects the distribution of AC in south China, but the impact is manifested during
233 warm events. Similarly, the effect of the NAO on the distribution of AC over central
234 China is only apparent during its negative phase.

235 The results suggest that if the occurrence of a negative polarity of NAO overlaps
236 with an El Niño event, the combined effects of the two may further worsen the AC over
237 eastern China. In contrast, a solo occurrence of a negative NAO event is associated with
238 above-normal AC over central China. Two cases, i.e., the co-occurrence of an El Niño
239 event and a negative NAO, and a solo negative NAO event, were chosen to further
240 explore the effect of the NAO and El Niño on the AC over China. From 1986-2006,
241 there are two years (1997 and 2002) with equivalent negative values of autumn NAOI
242 (-1.507 in 1997, and -1.510 in 2002). Winter 1997 corresponds with the strongest El
243 Niño in the past 120 years and winter 2002 corresponds with a neutral ENSO event.
244 Consequently, the anomalous distribution of AC during these two years are discussed
245 in the context of comparing the combined and solo effects of a negative NAO and El
246 Niño in impacting the distribution of AC over eastern China.

247 **3.3 Influences of the NAO & El Niño vs. the NAO on the AC**

248 Figure 5 presents the layer and column AC anomalies simulated for the winters of
249 1997 and 2002 departure from the climatological mean. Under the combined influence
250 of a negative NAO and El Niño (1997), positive aerosol concentration anomalies are
251 observed over eastern China (Fig. 5a, c). In addition, simulated enhanced AC were



252 observed over central China in winter 2002 under the impacts of a negative NAO (Fig.
253 5b, d). These characteristics are also apparent in the vertical distribution (Fig. 6), which
254 shows the zonal mean anomalies averaged over eastern China (105° – 120° E). For winter
255 1997, increased AC cover the whole eastern China, with maximum values
256 approximately 30° N, where the effects of the NAO and El Niño overlap (Figs. 4a, d).
257 The combined effects of the anomalies show a consistent distribution in the vertical
258 levels. In contrast, evident increased AC anomalies are seen in central China, with the
259 maximum at approximately 32° N during winter 2002.

260 The consistent results between the correlations and anomalies during the two cases
261 highlight the role of the negative NAO and El Niño events in determining the
262 distribution of AC over eastern China. The NAO shows a significant influence on the
263 central China AC that are only apparent during its negative phase, and the ENSO
264 impacts the AC over south China mainly during warm events.

265 **4. Mechanisms of the effects of the NAO and El Niño on the AC**

266 **4.1 Role of circulation transport**

267 The corresponding reverse role of the NAO and El Niño in impacting the
268 distribution of AC is mainly derived from their contrasting effects on circulation. Figure
269 7 shows the SLP and surface wind anomalies during the autumns of 1997 and 2002,
270 presenting an anomalously weak autumn NAO pattern. The negative phase of the NAO
271 displays as an anomalous SLP dipole structure between the middle latitude North
272 Atlantic Ocean and Arctic, i.e., with positive SLP anomalies at the Arctic over the



273 Atlantic sector, and anomalous negative SLP at middle latitude. The oscillation in the
274 SLP is connected with anomalies in the surface wind across the North Atlantic, i.e.,
275 associated with an anomalous cyclonic centered approximately 45°N and anti-cyclonic
276 circulation anomalies around Iceland. During boreal winter and spring, an anomalous
277 NAO could result in a tripole SST anomalous pattern in the North Atlantic Ocean
278 (Watanabe et al., 1999). A similar SST tripole pattern is observed during boreal autumn,
279 with warm SST anomalies at high and low latitudes, and negative SST anomalies at
280 middle latitudes in the North Atlantic sector (Fig. 8a, c). Note that the anomalous
281 negative SST during 1997 displays an east-west direction but originated from a
282 northwest-southeast direction during 2002 due to the different locations of anomalous
283 SLP (Fig. 7).

284 The North Atlantic anomalous SST tripole pattern is due to the feedback between
285 wind-SST, i.e., the anomalous anti-cyclonic (cyclonic) circulation weaken (strengthens)
286 the prevailing westerlies, which would result in decreased (increased) loss of heat and
287 warmer (cooler) anomalies in Ekman heat transport (Xie, 2004; Wu et al., 2009), and
288 is connected to cooler (warmer) local SST. Due to the short memory of the atmosphere,
289 the cross-seasonal influences of the NAO on the AC should be preserved in the
290 boundary layer forcing such as SST (Charney and Shukla, 1981). This anomalous
291 tripole SST pattern could persist to the following winter (Fig. 8b, d), as the anomalous
292 tripole SST pattern during winter and autumn show high consistencies in both 1997 and
293 2002, with significant spatial correlation coefficients of 0.32 and 0.51 between the
294 autumn and winter tripole SST patterns for 1997 and 2002, respectively.



295 Figure 9 shows the anomalous divergence at the upper troposphere. The
296 occurrence of a negative NAO phase is accompanied by an anomalous teleconnection
297 wave train over northern Eurasia (AEA) in the upper troposphere during boreal summer
298 (Li and Ruan, 2018). This anomalous teleconnection pattern is also observed during
299 boreal winter, with a shift in the precise locations. Under the influence of the anomalous
300 downstream teleconnection, north China is influenced by convergence anomalies, with
301 the center positioned over central China (Fig. 9). The anomalous convergence is clearly
302 seen in both the upper and lower troposphere, accompanied by anomalous easterlies or
303 southeasterlies over central China (Fig. 10). The direction of the anomalous wind is
304 opposite to the climatological winds, which would weaken the climatological wind and
305 is unfavorable for the transport of aerosol concentration, leading to increased AC over
306 central China, as displayed in Fig. 5.

307 For the winter 1997, corresponding to the El Niño's mature phase, south China
308 was influenced by an evident anomalous convergence at the lower troposphere,
309 indicating anomalous anticyclonic circulation over the coastal regions. Anomalous
310 southwesterlies prevailed in south China, implying weakened northerlies. That is the
311 anomalous meteorological conditions are unfavorable for aerosols transport in the
312 region and would result in a worsen air quality. In contrast, for the winter 2002, south
313 China was controlled by an anomalous divergence for that the main body of the WPSH
314 shifts to the south of south China (Fig. 10b). The anomalous circulation was favorable
315 for the emission of pollutant. Moreover, an evident anomalous divergence was observed
316 in south China in the winters of 1997 and 2002 at the upper troposphere; however, the



317 corresponding distribution of AC over this region is different. This highlights the role
318 of El Niño in impacting the circulation anomalies over south China, as mentioned above.
319 The occurrence of El Niño events would be accompanied by a northwest shift of the
320 WPSH during boreal winter and enhanced southwesterlies over south China (Weng et
321 al., 2009). Besides, column AC are mainly contributed by concentrations at lower
322 troposphere, suggesting that the lower troposphere circulation may play a vital role in
323 impacting the AC over south China.

324 **4.2 Role of wet deposit**

325 In addition to the contribution of the circulation anomalies to the distribution of
326 AC, changes in wet deposit also could affect distribution of AC. Figure 11 presents the
327 simulated wet deposit anomalies during the winters of 1997 and 2002. Negative
328 anomalies occurred over eastern China during the winter of 1997, favorable for
329 increased AC. This suggests the wet deposit plays a positive role in the enhanced AC
330 during winter 1997. Positive anomalies were observed over central China in the 2002
331 winter, inconsistent with the AC anomalies. The anomalous wet deposit during winter
332 of 1997 is paralleling to the AC anomalies over eastern China; however, not consistent
333 with that for the winter of 2002. This suggests that role of wet deposit in impacting the
334 AC over eastern China exists uncertainties, showing strong regional dependence. The
335 impact of wet deposit on the AC was examined by a sensitive experiment by turning
336 off the wet deposition (Fig. 11c-d). A similar anomalous AC distribution was observed
337 as those shown in Fig. 5, confirming that the role of wet deposit in impacting the
338 distribution of AC is not as important as the circulation.



339 5. Summary and Discussion

340 Using the simulations of GEOS-Chem model with fixed emissions, the
341 coordinated impacts of the previous autumn NAO and simultaneous ENSO on the
342 boreal winter AC over eastern China are investigated. The results present that both the
343 NAO and ENSO show asymmetry impacts on the boreal winter AC over eastern China,
344 i.e., the NAO manifests negative impacts over central China during its negative phase
345 and the ENSO positively impacts the AC over south China significantly during its warm
346 events. Consequently, the possible impacts of two cases were investigated to ascertain
347 the role of the NAO and ENSO on the distribution of AC over China. The winter 1997
348 had a co-occurrence of a negative NAO and an El Niño events, and winter 2002
349 corresponds to a negative NAO phase and neutral ENSO. For the winter 1997, obvious
350 enhanced AC were observed over eastern China, with a maximum approximately 30°N,
351 where the impacts of the NAO and El Niño overlap. For the winter 2002, there were
352 generally increased AC over central China. These results suggest that the co-occurrence
353 of a negative NAO and El Niño would worsen the air conditions over eastern China,
354 and a solo negative NAO is associated with increased AC over central China.

355 The cross-seasonal impacts of the preceding autumn NAO on the following winter
356 AC over China can be explained by the coupled air-sea bridge theory (Li and Ruan,
357 2018). The preceding negative NAO exhibits significant influences on the winds due to
358 the adjustment of the wind to the anomalous SLP. The associated anomalous wind could
359 affect the underlying regional SST, resulting in an anomalous SST tripole pattern over
360 the North Atlantic. Since the North Atlantic SST exhibit strong persistence, this



361 anomalous SST pattern could persist to the subsequent winter and inducing an
362 anomalous AEA teleconnection wave train in the upper troposphere, with anomalous
363 convergence over central China. Thus, central China is controlled by anomalous
364 southeasterlies or easterlies, which weaken the climatological northwesterlies and
365 induce increased AC over central China. In contrast, the occurrence of El Niño is linked
366 to warm SST anomalies over tropical eastern Pacific, by which the Rossby wave
367 activity would be altered (Wang et al., 2001; Feng and Li, 2011). A northwest shift of
368 the WPSH is seen during the winter of an El Niño event, associated with southwesterlies
369 anomalies over south China during the winter of 1997, indicating a weakening in the
370 climatological wind and leading to enhanced AC over south China. Therefore, the
371 high level of AC over eastern China during the winter 1997 results from the combined
372 role of the NAO and El Niño, and the high concentrations over central China in the
373 winter of 2002 are attributed to the NAO.

374 The possible reason for the asymmetric influence of the NAO on the AC was
375 further explored. When the autumn NAO is in the positive polarity, for example, two
376 positive cases of 1986 and 1992, the associated underlying SST anomalies (figure not
377 shown), particularly the tripole SST pattern, are not as evident as those shown in the
378 negative NAO. This result may provide a possible explanation for the asymmetric
379 relationship existed in the different phases of the NAO and AC, and implies the
380 complexity of the atmosphere-ocean feedback in the North Atlantic. This merits further
381 exploration related to why the linkage between the NAO and underlying SST is
382 nonlinear, and what process is responsible for their nonlinear relationship.



383 As noted above, the influence of the NAO on the AC only manifests during its
384 negative phase, and the impact of the ENSO is only significant during its warm events.
385 However, the relationship between the previous autumn and following winter ENSO is
386 insignificant, thus it is of interest to establish the nonlinear relationship among them
387 and investigate why there is strong asymmetry in the relationships. Zhang et al. (2015,
388 2019) explored the complex linkage between the boreal winter NAO and ENSO with
389 the former lagged for one month, indicating that the nonlinear relationship of the NAO
390 and ENSO is modulated by the interdecadal variation in the Atlantic Multi-Decadal
391 Oscillation. In addition, Wu et al. (2009) have illustrated the coordinated impacts of the
392 NAO and ENSO in modulating the interannual variation of the EASM; however, it has
393 not been shown to determine the AC yet. Therefore, it is of interest to further explore
394 whether the NAO and ENSO affect the AC over China in other seasons, as well as the
395 process involved. Furthermore, the present work is based on model simulations and due
396 to the limitations of the model simulations, only the interannual variations are
397 considered; as both NAO and ENSO show strong interdecadal variations, it is important
398 to determine their relationship over a longer period.

399 Moreover, the role of rainfall in influencing the AC shows uncertainties, i.e., a
400 positive effect over south China but not for central China. This result is similar with
401 that of Wu (2014), showing the impact of wet deposit on the AC shows regional and
402 seasonal dependence. In addition, the meteorological backgrounds of south China and
403 central China are different, baroclinic over central China and barotropic over south
404 China (Fig. 9 vs. 10), indicating the importance of climatology background in impacting



405 the spatial distribution of AC. In addition, both the NAO and ENSO show significant
406 correlations with AC over northwest China (Fig. 4); however, the interannual variation
407 (Fig. 2) and anomalies (Fig. 5) in AC over those regions are relatively small. Therefore,
408 the AC variation over those regions are not discussed.

409 Finally, the role of NAO and El Niño on the AC during boreal winter was
410 investigated based on GEOS-Chem simulations. The coordinated role of the NAO and
411 El Niño in affecting the distribution of AC over eastern China is highlighted by
412 comparing this effect with the solo role of the NAO. The result indicates that the
413 influence of meteorological factors impacting AC is complicated. Future work will
414 investigate the combined role of tropical and extratropical signals on seasonal AC to
415 better understand the variation across seasons and to determine the possible
416 contribution of natural variability to the current aerosol loading over China.

417



418 ***Author contribution***

419 J. F., J. L., and H. L. designed the research. J. F. and J. Z. performed the data
420 analysis and simulations. J. F. led the writing and prepared all figures. All the authors
421 discussed the results and commented on the manuscript.

422 ***Data availability***

423 Modeling results are available upon request to the corresponding author
424 (fengjuan@bnu.edu.cn).

425 ***Acknowledgement***

426 This work was jointly supported by the National Natural Science Foundation of
427 China (41790474 and 41705131).

428



References

- 429
- 430 Aw, J., and Kleeman, M. J.: Evaluating the first-order effect of intra-annual temperature
- 431 variability on urban air pollution, *J. Geophys. Res. Atmos.*, 108, D12, 4365,
- 432 <https://doi.org/10.1029/2002JD002688>, 2003.
- 433 Bey, I., Jacob, D. J., Yantosca, R. M., Logan, J. A., Field, B. D., Fiore, A. M., Li, Q. B.,
- 434 Liu, H. Y., Mickley, L. J., and Schultz, M. G.: Global modeling of tropospheric
- 435 chemistry with assimilated meteorology: Model description and evaluation, *J.*
- 436 *Geophys. Res.*, 106, 23073-23095, <https://doi.org/10.1029/2001JD000807>, 2001.
- 437 Cai, W. J., and Cowan, T.: La Niña Modoki impacts Australia autumn rainfall variability,
- 438 *Geophys. Res. Lett.*, 36, L12805, <https://doi.org/10.1029/2009GL037885>, 2009.
- 439 Chen, B. Q., and Yang Y. M.: Remote sensing of the spatio-temporal pattern of aerosol
- 440 over Taiwan Strait and its adjacent sea areas, *Acta Scientiae Circumstantiae*, 28, 12,
- 441 2597-2604, 2008.
- 442 Duan, F. K., He, K. B., Ma, Y. L., Yang, F. M., Yu, X. C., Cadle, S. H., Chan, T., and
- 443 Mulawa, P. A.: Concentration and chemical characteristics of PM_{2.5} in Beijing,
- 444 China: 2001-2002, *Sci. Total Environ.*, 355, 264–275,
- 445 <https://doi.org/10.1016/j.scitotenv.2005.03.001>, 2006.
- 446 Feng, J., and Li, J. P.: Influence of El Niño Modoki on spring rainfall over south China,
- 447 *J. Geophys. Res. Atmos.*, 116, D13102, <https://doi.org/10.1029/2010JD015160>,
- 448 2011.
- 449 Feng, J., Zhu, J. L., and Li, Y.: Influences of El Niño on aerosol concentrations over
- 450 eastern China, *Atmos. Sci. Lett.*, 17, 422-430, <https://doi.org/10.1002/asl.674>,



451 2016a.

452 Feng, J., Li, J. P., Zheng, F., Xie, F., and Sun, C.: Contrasting impacts of developing

453 phases of two types of El Niño on southern China rainfall, J. Meteorol. Soc. Jap.,

454 94, 359-370, <https://doi.org/10.2151/jmsj.2016-019>, 2016b.

455 Gong, D. Y., Wang, S. W., and Zhu, J. H.: East Asian winter monsoon and Arctic

456 Oscillation, Geophys. Res. Lett., 28, 2073-2076,

457 <https://doi.org/10.1029/2000GL012311>, 2001.

458 Hansen, J., Sato, M., and Ruedy, R.: Radiative forcing and climate response, J. Geophys.

459 Res., 102, D6, 6831-6864, <https://doi.org/10.1029/96JD03436>, 1997.

460 Harrison, D. E., and Larkin, N. K.: Seasonal U.S. temperature and precipitation

461 anomalies associated with El Niño: Historical results and comparison with 1997-

462 98, Geophys. Res. Lett., 25, 3959-3962, <https://doi.org/10.1029/1998GL900061>,

463 1998.

464 Hurrell, J. W.: Decadal trends in the North Atlantic Oscillation: Regional temperature

465 and precipitation, Science, 269, 676-679, doi:10.1126/science.269.5224.676, 1995.

466 IPCC, Climate change.: The physical science basis. Cambridge University Press.

467 Cambridge, UK, 2013.

468 Jeong, J. I., and Park, R. J.: Winter monsoon variability and its impacts on aerosol

469 concentrations in East Asia, Environ. Poll., 221, 285-292,

470 <https://doi.org/10.1016/j.envpol.2016.11.075>, 2017.

471 Jerez, S., Jimenez-Guerrero, P., Montavez, J. P., and Trigo, R. M.: Impact of the North

472 Atlantic Oscillation on European aerosol ground levels through local processes: a



473 seasonal model-based assessment using fixed anthropogenic emissions, Atmos.
 474 Chem. Phys., 13, 11195-11207, <https://doi.org/10.5194/acp-13-11195-2013>, 2013.

475 Jiang, Y. Q., Yang, X. Q., Liu, X. H., Yang, D. J., Sun, X. G., Wang, M. H., Ding, A. J.,
 476 Wang, T. J., and Fu, C. B.: Anthropogenic aerosol effects on East Asian winter
 477 monsoon: The role of black carbon-induced Tibetan Plateau warming, J. Geophys.
 478 Res. Atmos., 122, 5883-5902, <https://doi.org/10.1002/2016JD026237>, 2017.

479 Kalnay, E., Kanamitsu, M., Kistler, R., Colliins, W., Deaven, D., Gandin, L., Iredell,
 480 M., Saha, S., White, G., Woollen, J., Zhu, Y., Chelliah, M., Ebisuzaki, W., Higgins,
 481 W., Janowiak, J., Mo, K. C., Ropelewski, C., Wang, J., Leetmaa, A., Reynolds, R.,
 482 Jenne, R., and Joseph, D.: The NCEP/NCAR 40-Year Reanalysis Project, Bull.
 483 Amer. Meteor. Soc., 77, 437-472, [https://doi.org/10.1175/1520-](https://doi.org/10.1175/1520-0477(1996)077<0437:TNYRP>2.0.CO;2)
 484 [0477\(1996\)077<0437:TNYRP>2.0.CO;2](https://doi.org/10.1175/1520-0477(1996)077<0437:TNYRP>2.0.CO;2), 1996.

485 Karori, M. A., Li, J. P., and Jin, F. F.: The asymmetric influence of the two types of El
 486 Niño and La Niña on summer rainfall over southeast China, J. Climate, 26, 4567-
 487 4582, <https://doi.org/10.1175/JCLI-D-12-00324.1>, 2013.

488 Kleeman, M.: A preliminary assessment of the sensitivity of air quality in California to
 489 global change. Climate Change, 87, 273-292, [https://doi.org/10.1007/s10584-007-](https://doi.org/10.1007/s10584-007-9351-3)
 490 [9351-3](https://doi.org/10.1007/s10584-007-9351-3), 2008.

491 Li, J. P., and Ruan, C. Q.: The North Atlantic–Eurasian teleconnection in summer and
 492 its effects on Eurasian climates. Environ. Res. Lett., 13,
 493 <https://doi.org/10.1088/1748-9326/aa9d33>, 2018.

494 Li, J. P., and Wang, J. X. L.: A new North Atlantic Oscillation index and its variability,



- 495 Adv. Atmos. Sci., 20, 661-676, <https://doi.org/10.1007/BF02915394>, 2003.
- 496 Li, K., Liao, H., Cai, W. J., and Yang, Y.: Attribution of anthropogenic influence on
 497 atmospheric patterns conducive to recent most severe haze over eastern China,
 498 Geophys. Res. Lett., 45, 2072-2081, <https://doi.org/10.1002/2017GL076570>,
 499 2018.
- 500 Liao, H., Henze, D. K., Seinfeld, J. H., Wu, S. L., and Mickley, L. J.: Biogenic
 501 secondary organic aerosol over the United States: Comparison of climatological
 502 simulations with observations, J. Geophys. Res., 112,
 503 <https://doi.org/10.1029/2006JD007813>, 2007.
- 504 Liao, H., Chang, W., and Yang, Y.: Climatic effects of air pollutants over China: A
 505 review, Adv. Atmos. Sci., 32, 115-139, doi:10.1007/s00376-014-0013-x, 2015.
- 506 Liu, H., Jacob, D. J., Bey, I., and Yantosca, R. M.: Constraints from ²¹⁰Pb and ⁷Be on
 507 wet deposition and transport in a global three-dimensional chemical tracer model
 508 driven by assimilated meteorological fields, J. Geophys. Res., 106, 12109-12128,
 509 <https://doi.org/10.1029/2000JD900839>, 2001.
- 510 Lou, S. J., Russell, L. M., Yang, Y., Xu, L., Lamjiri, M. A., DeFlorio, M. J., Miller, A.
 511 J., Ghan, S. J., Liu, Y., and Singh, B.: Impacts of the East Asian monsoon on
 512 springtime dust concentrations over China, J. Geophys. Res. Atmos., 121, 8137-
 513 8152, <https://doi.org/10.1002/2016JD024758>, 2016.
- 514 Lou, S. J., Yang, Y., Wang, H. L., Smith, S. J., Qian, Y., Rasch, P. J.: Black carbon amplifies
 515 haze over the North China Plain by weakening the East Asian winter monsoon, Geophys.
 516 Res. Lett., 45, <https://doi.org/10.1029/2018GL080941>, 2018.



- 517 Mao, Y. H., Liao, H., and Chen H. S.: Impacts of East Asian summer and winter
518 monsoons on interannual variations of mass concentrations and direct radiative
519 forcing of black carbon over eastern China, Atmos. Chem. Phys., 17, 4799-4816,
520 <https://doi.org/10.5194/acp-17-4799-2017>, 2017.
- 521 Marshall, J., Johnson, H., and Goodman, J.: A study of the interaction of the North
522 Atlantic Oscillation with ocean circulation, J. Climate, 14, 1399-1421,
523 [https://doi.org/10.1175/1520-0442\(2001\)014<1399:ASOTIO>2.0.CO;2](https://doi.org/10.1175/1520-0442(2001)014<1399:ASOTIO>2.0.CO;2), 2001.
- 524 Moulin, C., Lambert, C. E., Dulac, F., and Dayan, U.: Control of atmospheric export of
525 dust from North Atlantic by the North Atlantic Oscillation, Nature, 387, 691-694,
526 <https://doi.org/10.1038/42679>, 1997.
- 527 Park, R. J., Jacob, D. J., Chin, M., and Martin, R. V.: Sources of carbonaceous aerosols
528 over the United States and implications for natural visibility, J. Geophys. Res., 108,
529 4355, <https://doi.org/10.1029/2002JD003190>, 2003.
- 530 Park, R. J., Jacob, D. J., Field, B. D., Yantosca, R. M., and Chin, M.: Natural and
531 transboundary pollution influences on sulfate-nitrate-ammonium aerosols in the
532 United States: implications for policy, J. Geophys. Res., 109, D15204,
533 <https://doi.org/10.1029/2003JD004473>, 2004.
- 534 Park, R. J., Jacob, D. J., Kumar, N., and Yantosca, R. M.: Regional visibility statistics
535 in the United States: natural and transboundary pollution influences, and
536 implications for the regional haze rule, Atmos. Environ., 40, 5405-5423,
537 <https://doi.org/10.1016/j.atmosenv.2006.04.059>, 2006.
- 538 Qin, Y., Chan, C. K., and Chan, L. Y.: Characteristics of chemical compositions of



539 atmospheric aerosols in Hongkong: spatial and seasonal distributions, Science of
540 the total Environment, 206, 25-37, [https://doi.org/10.1016/S0048-9697\(97\)00214-](https://doi.org/10.1016/S0048-9697(97)00214-3)
541 [3](https://doi.org/10.1016/S0048-9697(97)00214-3), 1997.

542 Qiu, Y. L., Liao, H., Zhang, R. J., and Hu, J. L.: Simulated impacts of direct radiative
543 effects of scattering and absorbing aerosols on surface-layer aerosol concentrations
544 in China during a heavily polluted event in February 2014, J. Geophys. Res., 122,
545 5955-5975, <https://doi.org/10.1002/2016JD026309>, 2017.

546 Rasmusson, E. M., and Carpenter, T. H.: Variations in tropical sea surface temperature
547 and surface wind fields associated with the Southern Oscillation/El Niño, Mon.
548 Wea. Rev., 110, 354-384, [https://doi.org/10.1175/1520-](https://doi.org/10.1175/1520-0493(1982)110<0354:VITSST>2.0.CO;2)
549 [0493\(1982\)110<0354:VITSST>2.0.CO;2](https://doi.org/10.1175/1520-0493(1982)110<0354:VITSST>2.0.CO;2), 1982.

550 Rayner, N. A., Parker, D. E., Horton, E. B., Folland, C. K., Alexander, L. V., and Rowell,
551 D. P.: Global analyses of sea surface temperature, sea ice, and night marine air
552 temperature since the late nineteenth century, J. Geophys. Res., 108, D14, 4407,
553 <https://doi.org/10.1029/2002JD002670>, 2003.

554 Ropelewski, C. F., and Halpert, M. S.: Global and regional scale precipitation patterns
555 associated with the El Niño/Southern Oscillation, Mon. Wea. Rev., 115, 1606-
556 1626, [http://dx.doi.org/10.1175/1520-0493\(1987\)115<1606:GARSPP>2.0.CO;2](http://dx.doi.org/10.1175/1520-0493(1987)115<1606:GARSPP>2.0.CO;2),
557 1987.

558 Singh, A., and Palazoglu, A.: Climatic variability and its influence on ozone and PM
559 pollution in 6 non-attainment regions in the United States, Atmos. Environ., 51,
560 212-224, doi:10.1016/j.atmosenv.2012.01.020, 2012.



- 561 Trenberth, K. E.: The definition of El Niño, Bull. Amer. Meteor. Soc., 78, 2771-2777,
562 [https://doi.org/10.1175/1520-0477\(1997\)078<2771:TDOENO>2.0.CO;2](https://doi.org/10.1175/1520-0477(1997)078<2771:TDOENO>2.0.CO;2), 1997.
- 563 Visbeck, M. H., Hurrell, J. W., Polvani, L., and Cullen, H. M.: The North Atlantic
564 Oscillation: past, present, and future, PNAS, 98, 12876-12877,
565 <https://doi.org/10.1073/pnas.231391598>, 2001.
- 566 Wang, B., Wu, R. G., and Fu, X. H.: Pacific–East Asian teleconnection: how does
567 ENSO affect East Asian Climate? J. Climate, 13, 1517-1536,
568 [https://doi.org/10.1175/1520-0442\(2000\)013<1517:PEATHD>2.0.CO;2](https://doi.org/10.1175/1520-0442(2000)013<1517:PEATHD>2.0.CO;2), 2000.
- 569 Wang, Y. H., Jacob, D. J., and Logan, J. A.: Global simulation of tropospheric O₃-NO
570 x-hydrocarbon chemistry 1. model formulation, J. Geophys. Res., 103, 10713,
571 <https://doi.org/10.1029/98JD00158>, 1998.
- 572 Watanabe, M., and Nitta, T.: Decadal changes in the atmospheric circulation and
573 associated surface climate variations in the Northern Hemisphere winter, J. Climate,
574 12, 494-509, [https://doi.org/10.1175/1520-0442\(1999\)012<0494:DCITAC>2.0.CO;2](https://doi.org/10.1175/1520-0442(1999)012<0494:DCITAC>2.0.CO;2), 1999.
- 576 Weng, H. Y., Behera, S. K., and Yamagata, T.: Anomalous winter climate conditions in
577 the Pacific rim during recent El Niño Modoki and El Niño events, Clim. Dyn., 32,
578 663-674, <https://doi.org/10.1007/s00382-008-0394-6>, 2009.
- 579 Wesely, M. L.: Parameterization of surface resistances to gaseous dry deposition in
580 regional-scale numerical models, Atmos. Environ., 23, 1293-1304,
581 [https://doi.org/10.1016/0004-6981\(89\)90153-4](https://doi.org/10.1016/0004-6981(89)90153-4), 1989.
- 582 Wu, R. G.: Seasonal dependence of factors for year-to-year variations of South China



583 aerosol optical depth and Hong Kong air quality, *Int. J. Climatol.*, 34, 3204-3220,
 584 doi:10.1002/joc.3905, 2014.

585 Wu, Z. W., Wang, B., Li, J. P., and Jin, F.-F.: An empirical seasonal prediction model of
 586 the east Asian summer monsoon using ENSO and NAO, *J. Geophys. Res.*, 114,
 587 D18120, <https://doi.org/10.1029/2009JD011733>, 2009.

588 Xie, S. P.: Satellite observations of cool ocean-atmosphere interaction, *Bull. Amer.*
 589 *Meteor. Soc.*, 85, 195-208, <https://doi.org/10.1175/BAMS-85-2-195>, 2004.

590 Xu, H. L., Feng, J., and Sun, C.: Impact of preceding summer North Atlantic Oscillation
 591 on early autumn precipitation over central China, *Atmos. Oceanic Sci. Lett.*, 6, 417-
 592 422, <https://doi.org/10.3878/j.issn.1674-2834.13.0027>, 2013.

593 Xuan, J., Liu, G. L., and Du, K.: Dust emission inventory in northern China, *Atmos.*
 594 *Environ.*, 34, 4565-4570, [https://doi.org/10.1016/S1352-2310\(00\)00203-X](https://doi.org/10.1016/S1352-2310(00)00203-X), 2000.

595 Yang, Y., Liao, H., Li, J.: Impacts of the East Asian summer monsoon on interannual
 596 variations of summertime surface-layer ozone concentrations over China, *Atmos.*
 597 *Chem. Phys.*, 14, 6867-6879, <https://doi.org/10.5194/acp-14-6867-2014>, 2014.

598 Yang, Y., Liao, H., and Lou, S. J.: Increase in winter haze over eastern China in the past
 599 decades: Roles of variations in meteorological parameters and anthropogenic
 600 emissions, *J. Geophys. Res. Atmos.*, 121, 13050-13065,
 601 <https://doi.org/10.1002/2016JD025136>, 2016.

602 Yang, Y., Russell, L. R., Lou, S. J., Liao, H., Guo, J. P., Liu, Y., Singh, B., and Ghan, S.
 603 J.: Dust-wind interactions can intensify aerosol pollution over eastern China,
 604 *Nature Comm.*, 8, 15333, <https://doi.org/10.1038/ncomms15333>, 2017.



- 605 Yue, X., and Unger, N.: Aerosol optical depth thresholds as a tool to assess diffuse
 606 radiation fertilization of the land carbon uptake in China, Atmos. Chem. Phys., 17,
 607 1329-1342, <https://doi.org/10.5194/acp-17-1329-2017>, 2017.
- 608 Zhang, L., Liao, H., and Li, J. P.: Impacts of Asian summer monsoon on seasonal and
 609 interannual variations of aerosols over eastern China, J. Geophys. Res., 115,
 610 D00K05, <https://doi.org/10.1029/2009JD012299>, 2010.
- 611 Zhang, R., Sumi, A., and Kimoto, M.: Impact of El Niño on the East Asian monsoon:
 612 A Diagnostic Study of the '86/87' and '91/92' events, J. Meteorol. Soc. Jpn., 74,
 613 49–62, https://doi.org/10.2151/jmsj1965.74.1_49, 1996. Zhang, R. H., Sumi, A.,
 614 and Kimoto, M.: A diagnostic study of the impact of El Niño on the precipitation
 615 in China, Adv. Atmos. Sci., 16, 229-241, <https://doi.org/10.1007/BF02973084>,
 616 1999.
- 617 Zhang, W. J., Wang, L., Xiang, B. Q., He, J. H.: Impacts of two types of La Niña on the
 618 NAO during boreal winter, Clim. Dyn., 44, 1351-1366,
 619 <https://doi.org/10.1007/s00382-014-2155-z>, 2015.
- 620 Zhang, W. J., Mei, X. B., Geng, X., Turner, A. G., and Jin, F.-F.: A nonstationary ENSO-
 621 NAO relationship due to AMO modulation, J. Climate, 32, 33-43,
 622 <https://doi.org/10.1175/JCLI-D-18-0365.1>, 2019.
- 623 Zheng, F., Li, J. P., Li, Y. J., Zhao, S., and Deng, D. F.: Influence of the Summer NAO
 624 on the Spring-NAO-Based Predictability of the East Asian Summer Monsoon, J.
 625 App. Meteorol. Climatol., 55, <https://doi.org/10.1175/JAMC-D-15-0199.1>, 2016.
- 626 Zhu, J. L., Liao, H., and Li, J. P.: Increases in aerosol concentrations over eastern China



627 due to the decadal-scale weakening of the East Asian summer monsoon, Geophys.
628 Res. Lett., 39(9), L09809, <https://doi.org/10.1029/2012GL051428>, 2012.
629 Zuo, J. Q., Li, W. J., Sun, C. H., Xu, L., and Ren, H. L.: Impact of the North Atlantic
630 sea surface temperature tripole on the East Asian summer monsoon, Adv. Atmos.
631 Sci., 30, 1173-1186, <https://doi.org/10.1007/s00376-012-2125-5>, 2013.
632



633 **Figure Captions:**

634 **Figure 1.** (a) The time series of the Niño3 index based on the GEOS-4 input skin
 635 temperature data for 1986-2006 ($^{\circ}\text{C}$). (b) is similar to (a) but is based on the
 636 HadISST. (c) The time series of the NAO index based on the GEOS-4 input sea
 637 level pressure. (d) is similar to (c) but is based on the NCEP/NCAR reanalysis.

638 **Figure 2.** The standard deviation of the simulated (a) surface layer $\text{PM}_{2.5}$ concentrations
 639 ($\mu\text{g}\cdot\text{m}^{-3}$) and (b) column burdens of $\text{PM}_{2.5}$ ($\text{mg}\cdot\text{m}^{-2}$) during boreal winter averaged
 640 from 1986 to 2006. (c) The horizontal distribution of boreal winter climatological
 641 mean wind at 850 hPa ($\text{m}\cdot\text{s}^{-1}$), shaded indicates the Tibetan Plateau.

642 **Figure 3.** (a) The spatial distribution of the correlation coefficients between surface
 643 layer $\text{PM}_{2.5}$ concentrations and the Niño3 index. (b) As in (a), but for the
 644 correlations with the NAOI. Color shading indicates a significant correlation at the
 645 0.1 level (0.37 is the critical value for significance at the 0.1 level).

646 **Figure 4.** Spatial distribution of the correlation coefficients between (a) positive and (b)
 647 negative Niño3 index values and surface-layer $\text{PM}_{2.5}$ concentrations. (c)-(d) as in
 648 (a)-(b), but for the NAOI. Color shading indicates a significant correlation at the
 649 0.2 level.

650 **Figure 5.** The spatial distribution of the simulated (left panel) surface layer $\text{PM}_{2.5}$
 651 concentrations ($\mu\text{g}\cdot\text{m}^{-3}$) and (right panel) column burdens of $\text{PM}_{2.5}$ ($\text{mg}\cdot\text{m}^{-2}$)
 652 during the boreal winters of 1997 (upper) and 2002 (below).

653 **Figure 6.** The pressure–latitude distribution of zonally averaged $\text{PM}_{2.5}$ anomalies over
 654 105° – 120°E during the winters of (a) 1997 and 2002 ($\mu\text{g}\cdot\text{m}^{-3}$).



655 **Figure 7.** The horizontal distribution of surface wind ($\text{m}\cdot\text{s}^{-1}$) and surface level pressure
 656 (hPa) based on the assimilated meteorological data during the autumns of (a) 1997
 657 and (b) 2002.

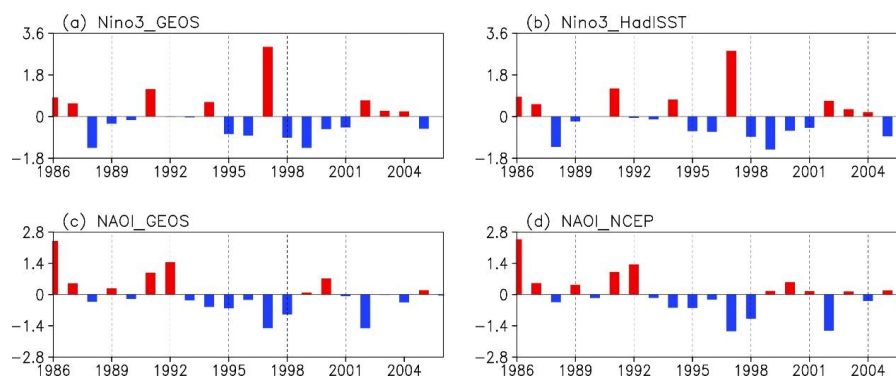
658 **Figure 8.** The horizontal distribution of skin temperature anomalies ($^{\circ}\text{C}$) based on the
 659 assimilated meteorological data during the (a) autumn and (b) winter of 1997. (c)-
 660 (d) As in (a)-(b), but during 2002.

661 **Figure 9.** Horizontal distribution of the divergence (10^{-5}s^{-1}) at 300 hPa during the
 662 winters of (a) 1997 and (b) 2002. The crosses denote the centers of action of the
 663 AEA pattern.

664 **Figure 10.** Horizontal distribution of 850 hPa wind anomalies (vectors; ms^{-1}) and
 665 divergence (shading; 10^{-5}s^{-1}) at 700 hPa during the winters of (a) 1997 and (b)
 666 2002.

667 **Figure 11.** The spatial distribution of the vertically integrated wet deposition flux
 668 anomalies during the winters of (a) 1997 and (b) 2002. (c)-(d), As in (a)-(b), but
 669 for the anomalous distribution of aerosol concentrations when the wet deposit is
 670 turned off.

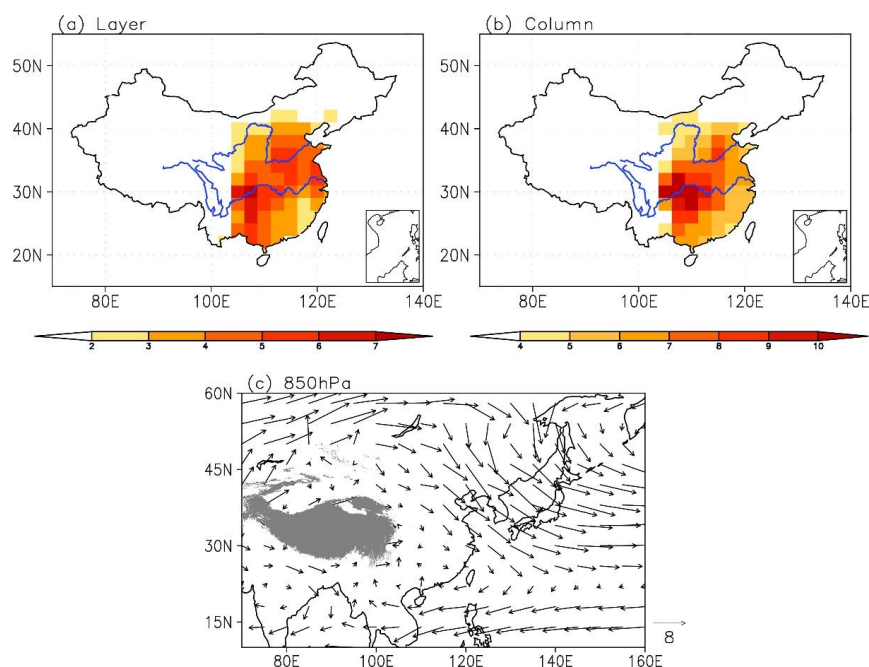
671



672

673 **Figure 1.** (a) The time series of the Niño3 index based on the GEOS-4 input skin
 674 temperature data for 1986-2006 (°C). (b) is similar to (a) but is based on the HadISST.
 675 (c) The time series of the NAO index based on the GEOS-4 input sea level pressure. (d)
 676 is similar to (c) but is based on the NCEP/NCAR reanalysis.

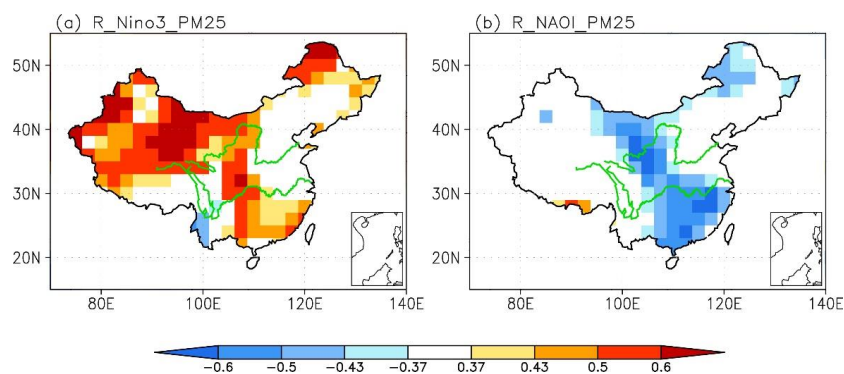
677



678

679 **Figure 2.** The standard deviation of the simulated (a) surface layer PM_{2.5} concentrations
 680 ($\mu\text{g}\cdot\text{m}^{-3}$) and (b) column burdens of PM_{2.5} ($\text{mg}\cdot\text{m}^{-2}$) during boreal winter averaged from
 681 1986 to 2006. (c) The horizontal distribution of boreal winter climatological mean wind
 682 at 850 hPa ($\text{m}\cdot\text{s}^{-1}$), shaded indicates the Tibetan Plateau.

683



684

685 **Figure 3.** (a) The spatial distribution of the correlation coefficients between surface
 686 layer PM_{2.5} concentrations and the Niño3 index. (b) As in (a), but for the correlations
 687 with the NAOI. Color shading indicates a significant correlation at the 0.1 level (0.37
 688 is the critical value for significance at the 0.1 level).

689

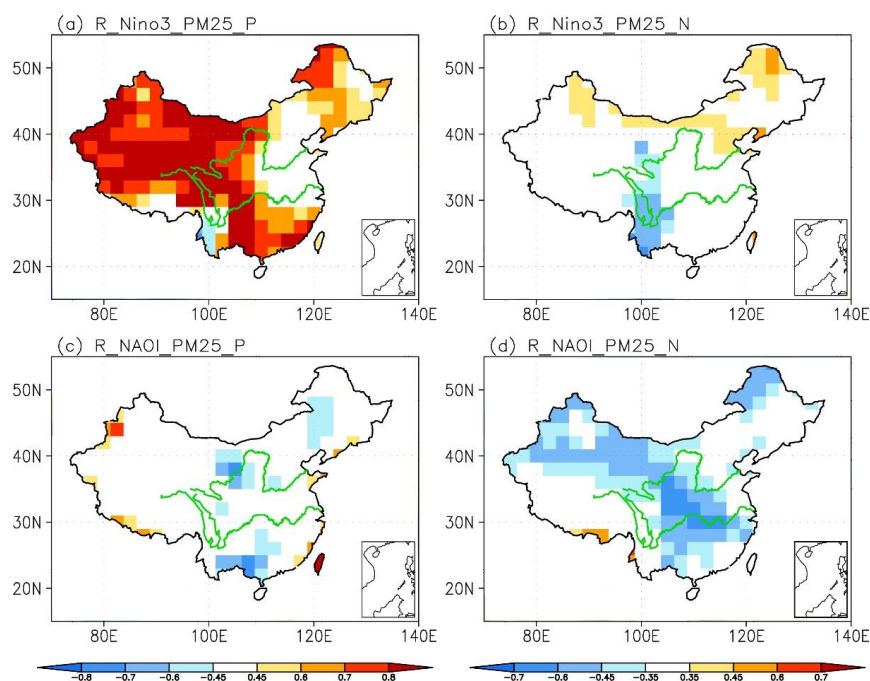


Figure 4. Spatial distribution of the correlation coefficients between (a) positive and (b) negative Niño3 index values and surface-layer PM_{2.5} concentrations. (c)-(d) as in (a)-(b), but for the NAOI. Color shading indicates a significant correlation at the 0.2 level.

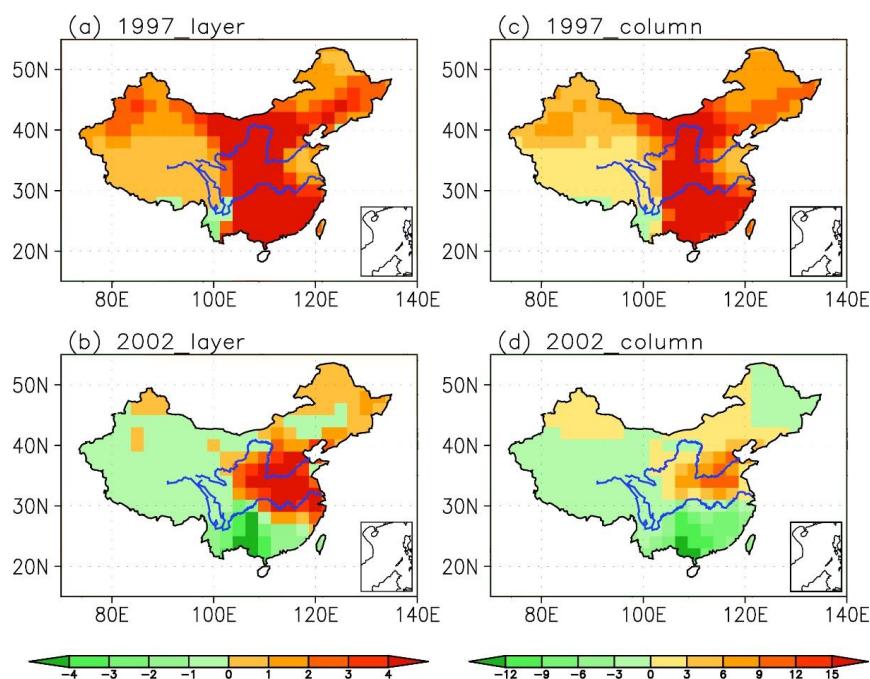


Figure 5. The spatial distribution of the simulated (left panel) surface layer $\text{PM}_{2.5}$ concentrations ($\mu\text{g}\cdot\text{m}^{-3}$) and (right panel) column burdens of $\text{PM}_{2.5}$ ($\text{mg}\cdot\text{m}^{-2}$) during the boreal winters of 1997 (upper) and 2002 (below).

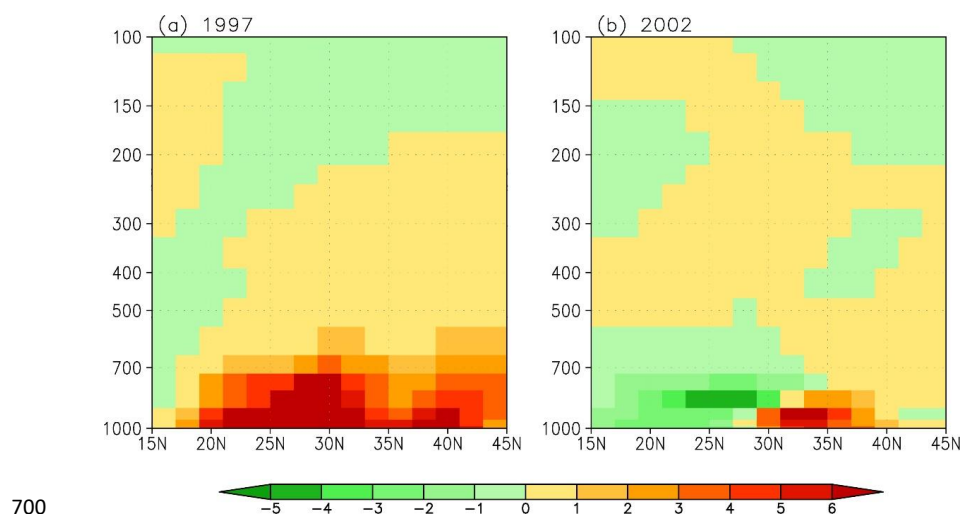


Figure 6. The pressure–latitude distribution of zonally averaged $\text{PM}_{2.5}$ anomalies over
 105°–120°E during the winters of (a)1997 and 2002 ($\mu\text{g}\cdot\text{m}^{-3}$).

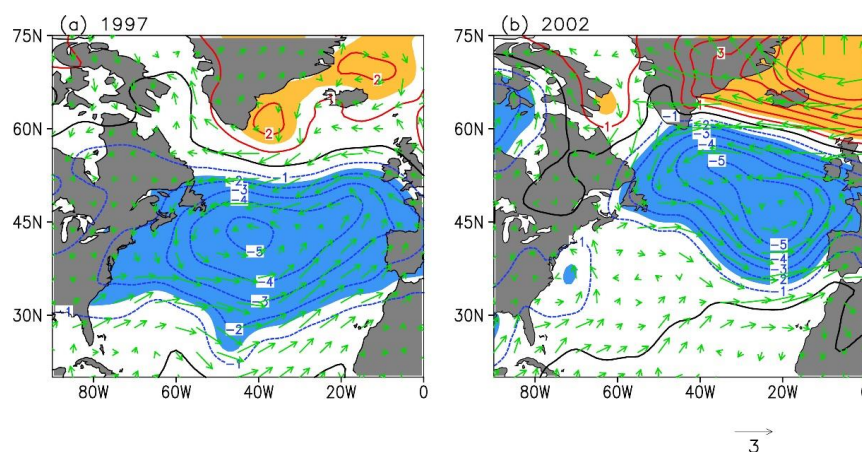
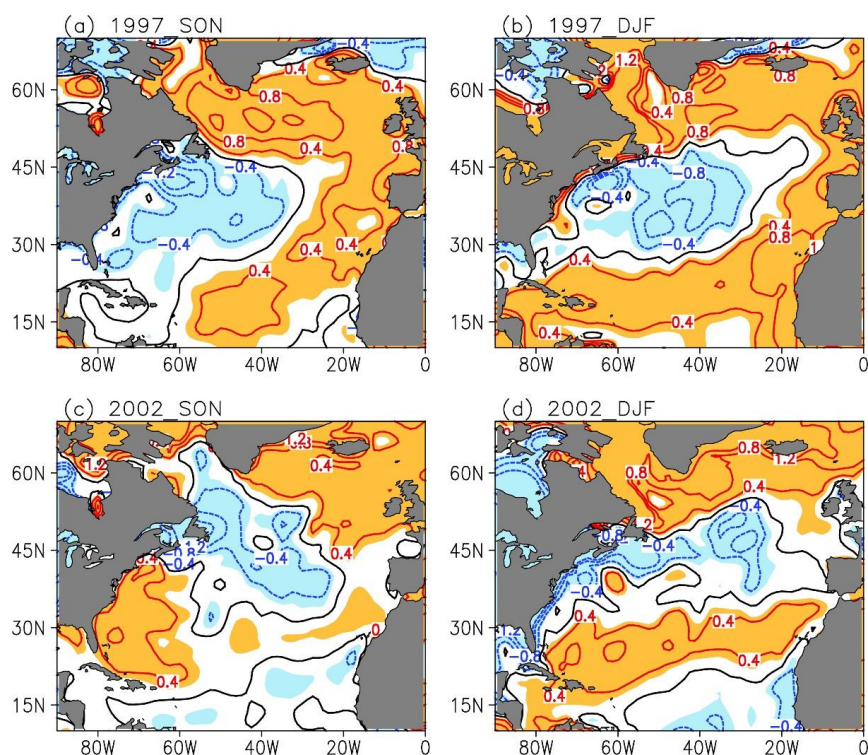


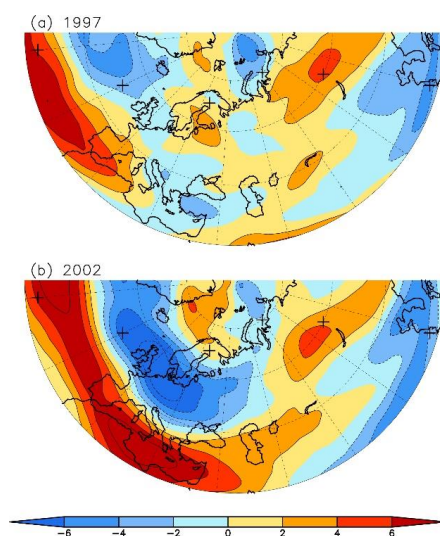
Figure 7. The horizontal distribution of surface wind ($\text{m}\cdot\text{s}^{-1}$) and surface level pressure (hPa) based on the assimilated meteorological data during the autumns of (a) 1997 and (b) 2002.



709

710 **Figure 8.** The horizontal distribution of skin temperature anomalies ($^{\circ}\text{C}$) based on the
 711 assimilated meteorological data during the (a) autumn and (b) winter of 1997. (c)-(d)
 712 As in (a)-(b), but during 2002.

713



714

715 **Figure 9.** Horizontal distribution of the divergence (10^{-5} s^{-1}) at 300 hPa during the
 716 winters of (a) 1997 and (b) 2002. The crosses denote the centers of action of the AEA
 717 pattern.

718

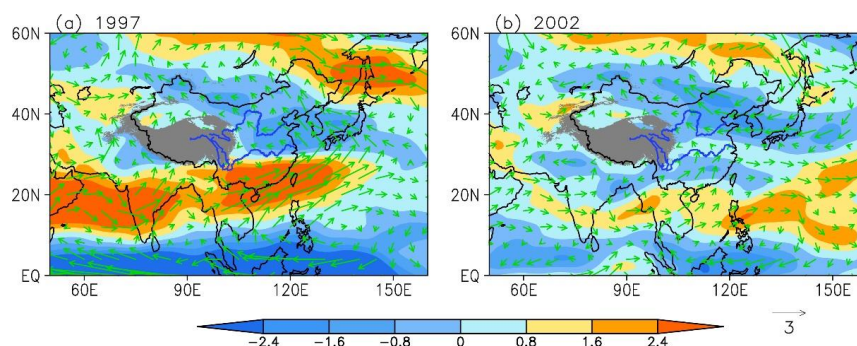
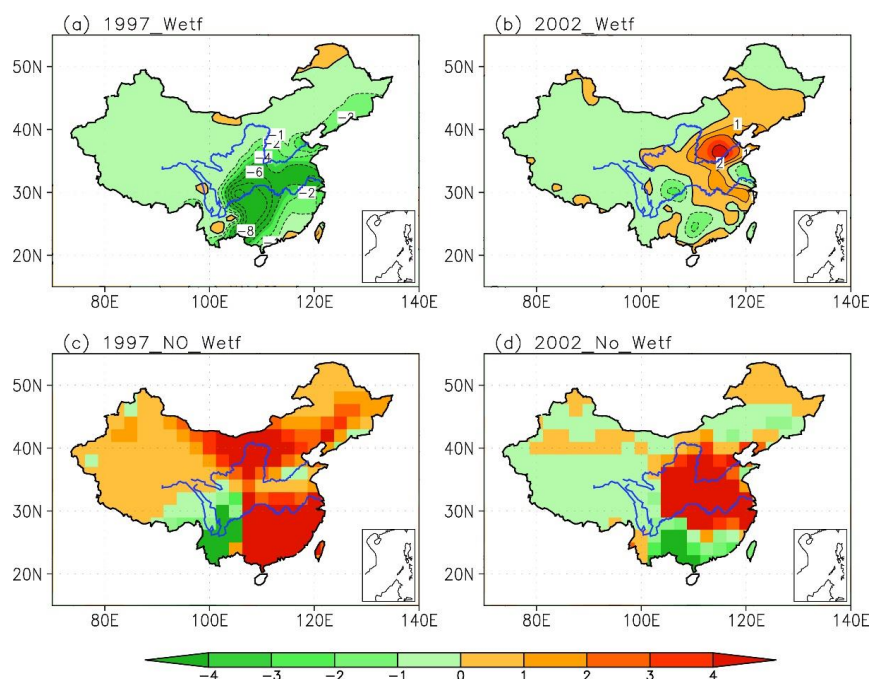


Figure 10. Horizontal distribution of 850 hPa wind anomalies (vectors; m s^{-1}) and divergence (shading; 10^{-5}s^{-1}) at 700 hPa during the winters of (a) 1997 and (b) 2002.



723

724 **Figure 11.** The spatial distribution of the vertically integrated wet deposition flux
 725 anomalies during the winters of (a) 1997 and (b) 2002. (c)-(d), As in (a)-(b), but for the
 726 anomalous distribution of aerosol concentrations when the wet deposit is turned off.